

Modeling of Digital Controllers in Electric Power System Dynamic Simulations

Mehran Jafari*, Gautier Bureau[†], Marco Chiaramello[†], Adrien Guironnet[†], Patrick Panciatici[†], and Petros Aristedou*

*Dept. of Electrical Eng., Computer Eng., & Informatics, Cyprus University of Technology, Limassol, Cyprus

[†]Réseau de Transport d'Électricité (RTE), France

Corresponding email: mm.jafari@edu.cut.ac.cy

Abstract—In modern electric power systems there are thousands of control devices, spanning from low-voltage distribution networks to high-voltage transmission networks, that manage the energy flows, ensure the secure operation and stabilize the system. To analyze the performance and assess the impact of controllers on the electricity grid, time-domain simulations are most frequently used. In recent decades, all the new controllers introduced in electric power systems are digital controllers and their analog counterparts are gradually being replaced. Nevertheless, many of the most frequently employed controllers are still modeled in time-domain simulations as analog (continuous) systems, employing transfer functions or differential-algebraic equations. This approach introduces a discrepancy between the real response of digital controllers and the simulated one. In this paper, we investigate the impact that correctly modeling digital controllers has on simulation accuracy and performance.

Index Terms—digital controllers, time-domain simulations.

I. INTRODUCTION

In recent decades, power systems are pushed to become more sustainable, reliable, and economic. This drive has led the electricity networks to operate closer to the security limits and increasingly rely on real-time, local or wide-area, controllers to ensure the reliability and resilience of the electricity supply. Large-scale dynamic simulations are often used to assess the security of power systems and to provide a digital twin for performing model-based design, tuning, or testing of the proposed controllers. Unlike static simulations or other mathematical assessment tools, dynamic simulations allow the incorporation of trajectory-based control and protection schemes into the analysis.

Due to the recent advancements and modernization of power systems, all modern control and protection devices are digital. Either implementing classical controls (such as a simple PI controller) or more advanced controllers based on artificial intelligence, optimization methods, or machine learning, there is a need to integrate these digital controllers into the large-scale dynamic simulations to assess the interaction between the devices and the system or the devices themselves. Nevertheless, their discrete nature makes them hard to embed in the continuous Differential-Algebraic Equation (DAE) simulation models used to represent the power system dynamics.

Digital controllers modeled either through their difference equations or even their actual control code incorporated into the power system DAE model leads to a hybrid DAE system

that is computationally intensive. Specifically, their discrete nature results in numerous discrete time-events (interruptions) in the simulation process, stagnation of it, and a limitation of the time-step size to the time between control events. Moreover, the hybrid nature of the system makes it impossible to use many of the classical analysis methods.

A frequently used approach is to employ a continuous equivalent of the digital controller [1]. This approach alleviates the time events and allows the use of classical analysis methods such as variable time-step methods that significantly accelerate the simulation performance. However, capturing the accurate response of digital controllers, along with their Analog-to-Digital (ADC) and Digital-to-Analog converters (DAC), in a continuous DAE simulation is difficult. In addition, the analog representation of digital controllers might conduct artificial problems that might not exist in the real system due to the Zero-Order-Hold (ZOH) time delays introduced. For instance, deadlocks in the simulation due to the limits imposed on controller variables – as in the case of the IEEE Anti-Windup (AW) controller shown in [2–4] – can arise. Another challenge is that not all digital controllers (e.g., optimization-based, artificial intelligence, etc.) have straightforward analog, equation-based, equivalents.

To address these challenges and provide insight to the modelling requirements for digital controllers, this paper:

- Investigates the challenges of modeling digital controllers in power system dynamic simulations.
- Investigates the impact of the sampling time of digital controllers on the power system dynamic results.
- Provides a comparison and discussion on the accuracy, modeling, and performance of digital controllers against their continuous equivalents.
- Investigates the impact of modelling on the deadlock situations observed in the IEEE AW PI model.

The rest of the paper is organized as follows. Section II discusses the different modeling formulation approaches for the controllers. Then, the numerical simulation of power systems and the incorporation of controller models are discussed in Section III. Three case studies are showcased in Section IV, followed by a discussion related to the accuracy and performance of the controllers in Section V. Finally, Section VI concludes the results and suggests future work.

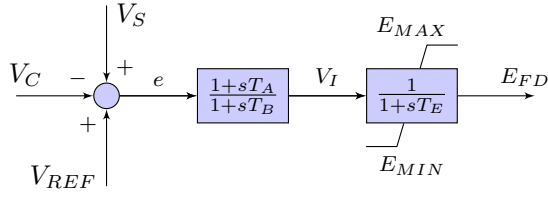


Fig. 1: Block diagram of SEXS controller

II. CONTROLLER MODELING

In this section, we describe the methods used for modeling controllers in power system time-domain simulations.

A. Block diagrams and transfer functions

The most common representation used in power systems literature and standards to explain the controller structure is through block diagrams due to their simplicity and clarity, e.g. [5, 6]. For instance, in Fig. 1 which is a simplified excitation system model (SEXS), it is easy to identify the inputs to the controller, the intermediate states, and their function.

Nevertheless, this simplicity has led many times to the models being implemented differently in the various simulation software and leading to discrepancies, where the system response is largely different between the various software. The reason is that the block diagrams rarely describe the exact implementation of limits (e.g., anti-windup integrator limits), selection flags, treatment of violations, etc. Several technical reports and standards have been revised to clarify the implementation of even simple and widespread control blocks (e.g., the IEEE AW integrator [4, 7, 8]).

This representation is closely related to the s -domain transfer functions of the various components that consist the controller. For instance, starting from the block diagram in Fig. 1, one can write the transfer function equations of the SEXS controller, assuming that the limits (E_{MIN} , E_{MAX}) are not reached, as:

$$E_{FD}(s) = \left(\frac{1 + sT_A}{1 + sT_B} \right) \left(\frac{1}{1 + sT_E} \right) e(s) \quad (1)$$

where $e(s)$ is the input and $E_{FD}(s)$ the output.

The block diagram and transfer function representations assume an input-output relationship, where the outputs are explicitly expressed in terms of the inputs. Such models follow a *causal* modeling standard [9] and the vast majority of general modeling languages for physical modeling have been based on this block-oriented paradigm.

B. Differential-algebraic equations

To avoid some of the issues associated with causal models and to be able to easier incorporate the controllers into large-scale power system dynamic simulation software (see Section III), an acausal approach can be used where models essentially are expressed in terms of undirected DAEs. This makes them much more reusable and composable, addressing some of the challenges of large-scale modeling and simulation,

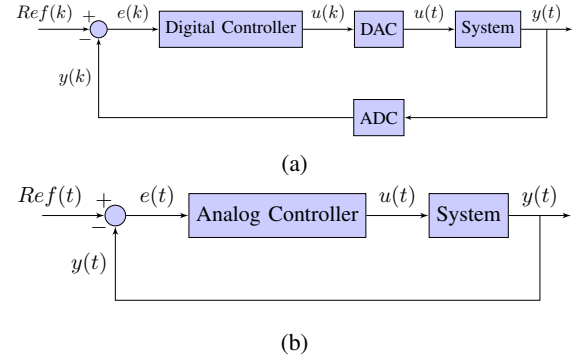


Fig. 2: Interface of controllers in a (a) hybrid and (b) continuous system analysis

and is the paradigm chosen in recent modeling languages, such as Modelica [10]. For instance, (1) can be converted to:

$$\begin{aligned} T_E \dot{E}_{FD}(t) &= V_I(t) - E_{FD}(t) \\ T_B \dot{V}_t(t) &= e(t) - V_t(t) \\ 0 &= T_A e(t) + (T_B - T_A) V_t(t) - T_B V_I(t) \end{aligned} \quad (2)$$

where $V_t(t)$ is a temporary variable.

It can be seen that the notion of input-output has been removed from this representation.

C. Discrete domain and difference equations

The majority of the controllers today are digital and to perform model-based control design or to assess the performance, security, and stability of the analyzed systems, a hybrid analysis (such as the one in Fig. 2a) needs to be performed. The ADC samples some of the controlled system variables ($y(t)$) with a sampling time T_s and feeds back to the digital controller the discrete samples ($y(k)$). The discrete controller output ($u(k)$) is then fed to the DAC to be converted to a continuous signal that drives the controlled system. In most practical applications, the DAC is usually a ZOH model.

The discrete domain representation of a controller can be easily computed from the continuous domain transfer function using one of the several available discretization methods, like ZOH, First-Order-Hold, Forward/Backward Difference, or Trapezoidal method (Tustin's approximation). For instance, applying the Backward Difference method to (1), provides:

$$E_{FD}(z) = \frac{zT_s(z(T_s + T_A) - T_A)}{(z(T_s + T_B) - T_B)(z(T_s + T_E) - T_E)} e(z) \quad (3)$$

Consequently, to be implemented in a digital controller, the difference equations are more useful:

$$\begin{aligned} E_{FD}(k+1) &= \frac{1}{(T_s + T_B)(T_s + T_E)} [E_{FD}(k)(T_E(T_s + 2T_B) \\ &\quad + T_s T_B) - E_{FD}(k-1)(T_B T_E) \\ &\quad + e_{(k+1)}(T_s(1 + T_A)) - e_{(k)}(T_s T_A)] \end{aligned} \quad (4)$$

computed at time $t = t_k = kT_s$ and held constant over the period $t \in [kT_s, (k+1)T_s)$ (assuming a ZOH DAC). These

equations are then usually implemented in the control-loop of the digital controller hardware.

III. POWER SYSTEM NUMERICAL SIMULATIONS

Due to the complexity and non-linear nature of electric power systems, time-domain numerical simulations are most frequently used to assess their security. Thus, the physical system is modeled with a set of index-1 DAEs [11] that notably incorporate the network, generation, and load dynamics. The compact form of the problem is characterized by:

$$F(\dot{x}, x, y, p) = 0 \quad (5)$$

where x are the differential, y the algebraic variables, and p the parameters of the system. The DAE system is then discretized using an integration method (e.g., trapezoidal method, BDF, etc.) and solved over a time horizon.

The power system DAE models are hybrid in nature, with discrete events (either discrete state or time events) impacting the time-step selection and the DAE. More specifically, time events take place at specific time instances (e.g., a predefined fault) while state events depend on the simulation trajectory and are not known beforehand (e.g., a generator reaching the output limit) [12]. In both cases, when a discrete event takes place, the time-step h is usually reduced to match the event time and the impact of the discrete change on the DAEs is reflected before continuing with the simulation.

To perform model-based control design or to assess the security of the system under the control actions, the latter need to be connected to the continuous-time physical system (5). When a digital controller is concerned, the most accurate representation is the one of Fig. 2a. In this case, the DAC and ADC models need to be correctly modeled and the digital controller difference equations (e.g., (4)) provide the control law. There are two issues with this approach.

First, the digital control output is updated at each T_s (for most power system applications ranges from few milliseconds to several seconds). This introduces a discrete time event at each sampling instance, which usually leads to reduced time steps and increased simulation time. This issue has higher impact on variable time-step methods (as the time-step gets "stuck") and when the system has multiple digital controllers (thus, thousands of discrete time events are introduced). Second, the hybrid representation makes it impossible to use classical control design methods or stability assessment methods (e.g., eigenvalue analysis), thus requiring work with discrete control design methods.

Alternatively, a continuous-time equivalent of the digital controller can be used, as shown in Fig. 2b. Usually, the DAE representation of the controller is used (e.g., (2)) that is easy to incorporate in the power system model (5). This approach alleviates the two issues mentioned above, as the continuous-time equivalent can be handled as the rest of the system DAEs. However, it also introduces new challenges.

First, to ensure that the continuous and discrete controllers have the same response, the effect of the ZOH DAC needs to be appropriately incorporated into the system. This is

usually done with the use of some Padé approximates whose parameters depend on the T_s of each controller. In turn, this results in a Delay Differential-Algebraic Equations system (DDAE).

Second, while the time events due to the T_s of the digital control are not an issue anymore, there is a need to detect and treat state events related to the controller limits (e.g., $E_{MIN/MAX}$ in Fig. 1). In the real digital controller implementation, the detection, location, and treatment of limits are easy and straightforward due to the ZOH. However, in the continuous equivalents, there is a need to detect, locate, and treat the limits through state events [13]. The implementation is not straightforward and can create artificial (that would never appear in the real digital controller) deadlocks. Several papers have been published analyzing methodologies for the implementation and treatment of the control limits in continuous controllers, which become irrelevant in real-world digital control implementations [2, 14].

Third, many of the modern digital controllers are not DAE-based and cannot possibly be incorporated in (5). Receding-horizon or one-shot optimization-based controllers, artificial intelligence-based, Neural-Network (NN) or Deep NN controllers are some of the modern digital controls incorporated in power systems. In these cases, the use of a hybrid system (see Fig. 2a) is mandatory.

Finally, when comparing the two approaches in Fig. 2, we can consider i) the ability of the system to capture the digital controller behavior (e.g., if a DAE-based equivalent can even be formulated), ii) the accuracy of the simulated results with the hybrid analysis (Fig. 2a) as the reference, and iii) the computational burden. In the following section, these considerations will be showcased through some case studies.

IV. SIMULATION RESULTS

For all the simulations, a predictor-corrector integration method consisting of a pair of second-order Adams-Bashford (explicit) and second-order Adams-Moulton (implicit) is utilized. Also, the step size for all simulations is fixed and equal to 1 ms unless otherwise specified. The sampling time of the digital controllers is chosen to be an integer multiple of the time step. Finally, a uniform quantization of 16 bits is used for the ADC and ZOH DAC.

First, the IEEE 421.5-2016 AW PI controller is tested in an open-loop and closed-loop setting, comparing an analog implementation to a digital one with several different time-sampling parameters. Then, a 3-bus system with an AVR and a governor is simulated, with similar comparisons.

A. PI controller formulation

The IEEE 421.5-2016 AW PI controller (see Section E.5 in [6]) formulated as a DAE model (see Section II-B), including the limits, is given by:

$$\begin{aligned} \text{If } y &\geq w_{max} : w = w_{max} \quad \text{and} \quad \dot{x} = 0 \\ \text{If } y &\leq w_{min} : w = w_{min} \quad \text{and} \quad \dot{x} = 0 \\ \text{Otherwise } &\dot{x} = k_i u \quad \text{and} \quad w = y = k_p u + x \end{aligned} \quad (6)$$

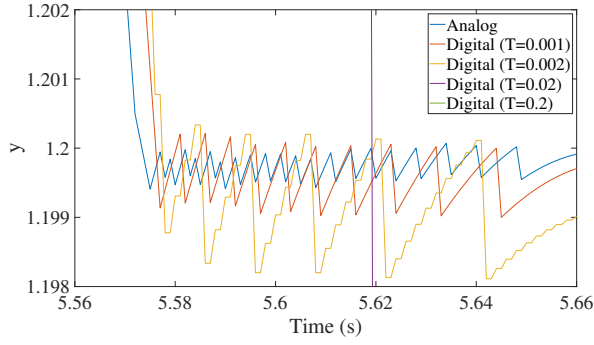


Fig. 3: Results of simulation of the digital AW PI controller with different sampling times between 5.56 to 5.66 s

Discretizing the controller using the Forward Difference method and a sampling time T , leads to:

$$\text{If } y_k \geq w_{max} : w_{k+1} = w_{max} \quad \text{and} \quad x_{k+1} = x_k$$

$$\text{If } y_k \leq w_{min} : w_{k+1} = w_{min} \quad \text{and} \quad x_{k+1} = x_k$$

$$\text{Otherwise } x_{k+1} = k_i u_k T + x_k \quad \text{and}$$

$$w_{k+1} = y_{k+1} = k_p u_{k+1} + x_{k+1} \quad (7)$$

B. Open-loop PI controller

First, a simple open-loop example is shown where the input u is varied over a 6.5 seconds horizon as (8). The input drives the controller over the upper limit and then returns to remain exactly on the limit. The parameters of the controllers are set to $k_i = 3$ and $k_p = 1$ and the limits are set to $w_{min} = -1.2$ and $w_{max} = 1.2$.

$$\text{If } t < 3 : \dot{u}(t) = 1; \quad \text{Else} : \dot{u}(t) = -1 \quad (8)$$

Since the sampling time of the controller is equal to the time-step size, the simulation result for the continuous and digital controller with $T = 0.001$ is identical. This is because the analog controller in (6) is discretized by the integration method and updated at each time step $h = 0.001$ s. Thus, the update of both the analog and the digital output is identical at 1 ms.

Variable y is illustrated in Fig. 3 for different sampling times of the digital controller, and for the period between 5.56 – 5.66 s shows that a sampling time higher than the step size can change its response. This is because the continuous controller equations (6) are updated every time step ($h = 1$ ms) while the difference equations of the digital controller (7) every time-sampling $T > h$.

Fig. 3 was selected to showcase the chattering phenomenon reported in [7]. It can be seen that the chattering is still present in all models with variations in its amplitude due to the sampling time. Nevertheless, looking at Fig. 4, which shows the number of Newton iterations required for both the continuous and digital controllers, the computational performance of the digital controllers is much better. Also, the possibility of a deadlock happening in the digital controller models is non-existent. This is because the limits are updated with a

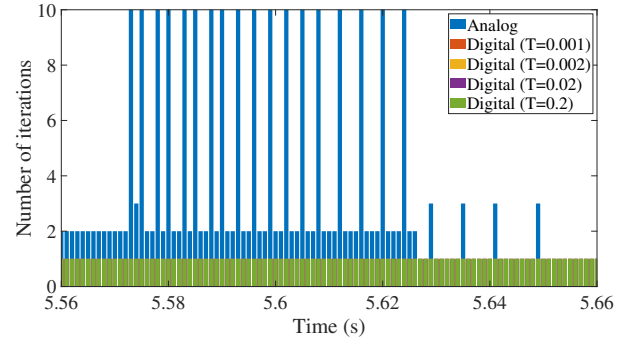


Fig. 4: Number of Newton iterations for the continuous and digital AW PI controller with different sampling times between 5.56 to 5.66 s (all digital controllers have only one iteration)

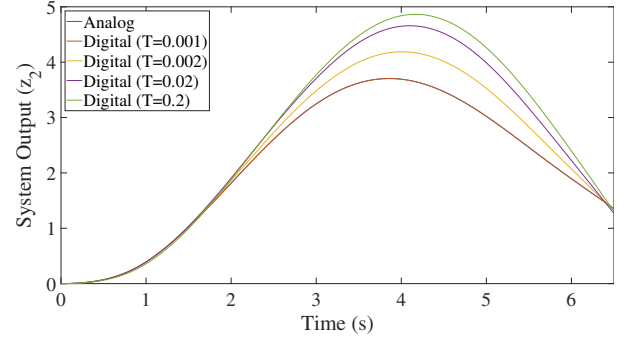


Fig. 5: System's output z_2 for the analog and digital controllers with different sampling times (first scenario)

ZOH approach that introduces a time-delay, as explained in Section III.

C. Closed-loop PI controller

In this case study, the PI controller is used to drive a simple continuous system of two differential equations:

$$\begin{bmatrix} \dot{z}_1 \\ \dot{z}_2 \end{bmatrix} = \begin{bmatrix} a & b \\ -b & 0 \end{bmatrix} \begin{bmatrix} z_1 \\ z_2 \end{bmatrix} + \begin{bmatrix} -b \\ 0 \end{bmatrix} w \quad (9)$$

All the parameters of the controller are kept the same and $k_f = 0.1$. In addition, the continuous system parameters are set to $a = -0.1$ and $b = 0.9$.

First, the same variation dictated by (8) is applied. The output z_2 of the system is illustrated in Fig. 5 for analog and digital controllers with different sampling times. For $T \leq h$, the response is identical. However, a significant difference is observed for $T > h$.

In the second scenario, a step change is applied to $u = 0 \rightarrow 1$ with $k_p = 2$, $k_i = 1$, $k_f = 1$, $a = -0.2$, $b = 0.9$, $w_{min} = -1.1$, and $w_{max} = 1.1$. The response is illustrated in Fig. 6 and the controllers' output in Fig. 7, respectively. It can be seen that even in this simplified LTI ODE system, a change in the sampling time T can provide different simulation results. In addition, the activation and deactivation of the limits are shifted according to the sampling time.

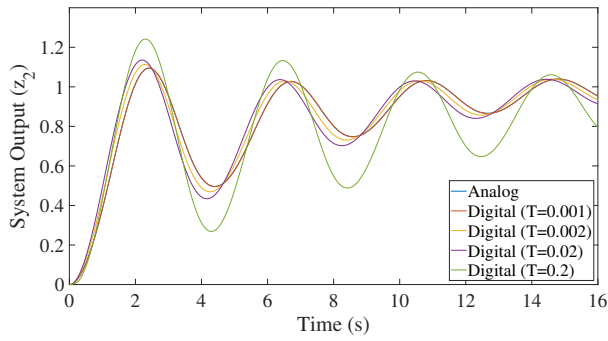


Fig. 6: System's output z_2 for the analog and digital controllers with different sampling times (second scenario)

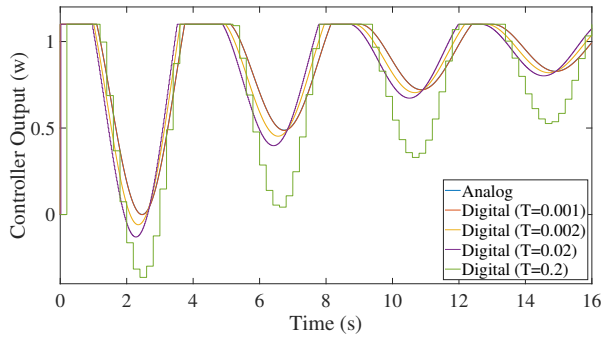


Fig. 7: Controller's output w for the analog and digital controllers with different sampling times (second scenario)

TABLE I: Performance of simulations for the analog and digital controllers with fixed and variable time steps

Method	Nb. Newton iterations	Runtime (s)
Analog cont. - fixed time steps	31580	16.94
Analog cont. - variable time steps	436	0.34
Digital cont. - fixed time steps	31717	13.77
Digital cont. - variable time steps	3422	1.69

D. Three-bus system

In this case study, we employ a 3-bus network, illustrated in Fig. 8, consisting of a synchronous generator (SG), a photovoltaic (PV), and a load connected by two transmission lines. The dynamics of the generator are under the control of an AVR (IEEE DC2A) [6] and a governor (type HYG0V) [5] with sampling time T_G and T_E , respectively. A typical sampling time for the digital AVR is usually from 5-50 ms [15] and the governor 5-250 ms [16], depending on the controller and the system type.

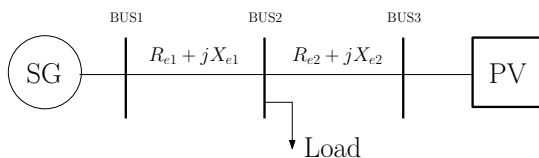


Fig. 8: The schematic of the 3-bus network

The simulation of a step change in PV's active power production from 3 to 2 MW between seconds 3 to 6 is implemented. The system is simulated first with the analog representation of the controllers using a fixed time-step ($h = 1$ ms) and a variable time-step ($h_{min} = 1$ ms and $h_{max} = 500$ ms). Then, the simulation is repeated for the hybrid system.

The results for the voltage of Bus 2, the generator speed deviation, the governor, and the exciter output are depicted in Figs. 9-11. The simulations with the analog controller variants give an identical response, both for the variable time-step and the constant time step versions. The hybrid simulation deviates from the analog ones, with the ZOH shown more prominent in Fig. 10. The performance comparison is briefed in Table I. It can be seen that the performance of the analog controller simulation with the variable time step integration is better than the one with the digital controllers due to the bigger time steps taken. This is one of the main reasons that analog controllers are preferred in dynamic simulations.

V. DISCUSSION

In this section, the most important observations are summarized, and associated verdicts are discussed.

A. Accuracy

Based on the results in Section IV, it can be observed that in most cases the accuracy between simulating an analog or a digital controller (having the digital controller as the benchmark) is impacted severely by the sampling time. When the sampling time is smaller than the time step ($T < h$) the trajectories are identical between the two, while with a sampling time larger than the time step ($T > h$) there is a notable discrepancy. This is due to the fact that the controller modeled as continuous with a DAE is discretized by the integration method and updated according to the time step, while the digital controller has a pre-defined sampling time and is interfaced to the rest of the system with a DAC.

Furthermore, although using a variable step size method helps with the performance of systems controlled by continuous controllers, it results in slightly lower accuracy (due to the allowance of higher time steps). However, it doesn't affect the digital controllers' accuracy significantly, since the step size is limited to the biggest difference between the sampling time of the digital controllers.

B. Performance

In the case of using a variable step size solver (see Section IV-D), the continuous models outperform the digital ones since no step size reduction is imposed. When a hybrid model is used, the time step is always limited to the biggest difference between the digital controller sampling times (time events).

On the other hand, when the continuous controller model is used, there is a need for detecting and locating the state events introduced due to the controller limits. When the digital controller model is used, this is not necessary due to the delays introduced by the ZOH. Thus, even if higher time-steps can be implemented with the continuous models, a zero-crossing detection algorithm needs to be implemented.

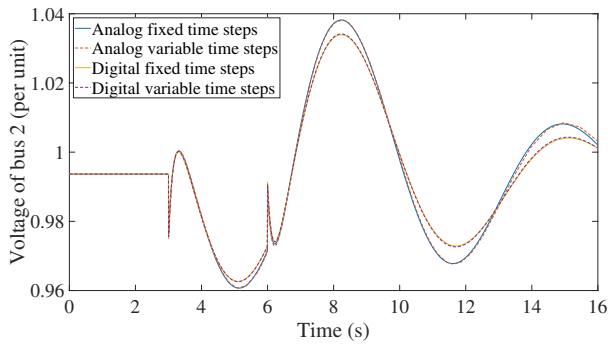


Fig. 9: Voltage of the load Bus 2

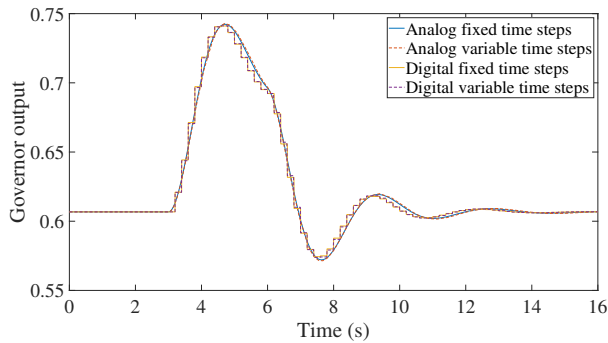


Fig. 10: Output signal of the governor

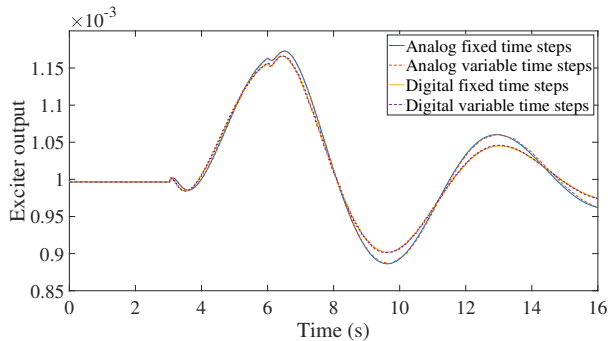


Fig. 11: Output signal of the exciter

C. Modeling

To model the controllers as continuous devices requires their equations to be accessible and differentiable. This means that heuristic (and other non-equation-based) controllers can not be included and numerically solved. However, in the case of digital controllers, due to the time-delays introduced by the ZOH and since their equations don't appear in the solver, they can be treated as a black box with an input and output that is called before each time step.

Finally, it is shown that although chattering problems still exist for the digital controller models, deadlocks cannot happen. Therefore, in the case of deadlock problems, the performance of the digital controller is much better in the deadlock zone as the solver doesn't stagnate.

VI. CONCLUSION

In this paper, different approaches for modeling the controller in power systems were briefly reviewed and a comparison between the analog and digital modeling of controllers in power system dynamic simulations was provided through case studies.

In this paper, it was shown that there are several differences related to accuracy, performance, and modeling aspects. Overall, implementing the real digital controller is better in all aspects, except the reduced performance caused by the limit on the time-step size introduced by the sampling times (discrete time-events). This problem can be alleviated by proposing and implementing new methods that can help to embed the digital controllers in the dynamic simulations without causing the solvers to reduce the time-step size, which is still an open challenge.

REFERENCES

- [1] J. V. Wallbank, S. Singh, and S. Walters, "An introduction to the implementation of digital control — leading to the control of electrical power systems," in *2017 52nd International Universities Power Engineering Conference (UPEC)*, 2017, pp. 1–5.
- [2] I. A. Hiskens, "Dynamics of type-3 wind turbine generator models," *IEEE Transactions on Power Systems*, vol. 27, no. 1, pp. 465–474, 2011.
- [3] —, "Trajectory deadlock in power system models," in *2011 IEEE International Symposium of Circuits and Systems (ISCAS)*. IEEE, 2011, pp. 2721–2724.
- [4] H. Cui, Y. Zhang, F. Milano, and F. Li, "On the modeling and simulation of anti-windup proportional-integral controller," *arXiv preprint arXiv:2005.05430*, 2020.
- [5] IEEE Power System Dynamic Performance Committee, "Dynamic models for turbine-governors in power system studies," IEEE, Tech. Rep., 2013.
- [6] "IEEE Recommended Practice for Excitation System Models for Power System Stability Studies," *IEEE Std 421.5-2016*, pp. 1–207, 2016.
- [7] M. A. A. Murad, B. Hayes, and F. Milano, "Application of Filippov theory to the IEEE Standard 421.5-2016 anti-windup PI controller," in *2019 IEEE Milan PowerTech*. IEEE, 2019, pp. 1–6.
- [8] M. A. A. Murad and F. Milano, "Modeling and simulation of pi-controllers limiters for the dynamic analysis of vsc-based devices," *IEEE Transactions on Power Systems*, vol. 34, no. 5, pp. 3921–3930, 2019.
- [9] G. Schweiger, H. Nilsson, J. Schoeggel, W. Birk, and A. Posch, "Modeling and simulation of large-scale systems: A systematic comparison of modeling paradigms," *Applied Mathematics and Computation*, vol. 365, p. 124713, 2020.
- [10] S. Mattsson, H. Elmqvist, and M. Otter, "Physical System Modeling with Modelica," in *Control Engineering Practice*, vol. 6, no. 4, 1998, pp. 501–510.
- [11] F. Milano, *Power System Modelling and Scripting*, ser. Power Systems. Springer Berlin Heidelberg, 2010.
- [12] D. Fabozzi, A. S. Chieh, P. Panciatici, and T. Van Cutsem, "On simplified handling of state events in time-domain simulation," *Proceedings of the 17th PSCC*, 2011.
- [13] C. W. Gear and O. Osterby, "Solving ordinary differential equations with discontinuities," *ACM Transactions on Mathematical Software (TOMS)*, vol. 10, no. 1, pp. 23–44, 1984.
- [14] M. A. A. Murad and F. Milano, "Chattering-free modelling and simulation of power systems with inclusion of filippov theory," *Electric Power Systems Research*, vol. 189, p. 106727, 2020.
- [15] K. Hirayama, Y. Tone, K. Takagi, H. Murakami, M. Shibata, H. Nagamura, and Y. Takagi, "Digital AVR application to power plants," *IEEE Transactions on Energy Conversion*, vol. 8, no. 4, pp. 602–609, 1993.
- [16] S. C. Tripathy, "Digital speed governor for steam turbine," *Energy conversion and management*, vol. 35, no. 2, pp. 159–169, 1994.